

# The stability of a cubic fixed point in three dimensions from the renormalization group

K. B. Varnashev\*

Department of Physical Electronics, Saint Petersburg Electrotechnical  
University,  
Professor Popov Street 5, St.Petersburg, 197376, Russia

## Abstract

The global structure of the renormalization-group flows of a model with isotropic and cubic interactions is studied using the massive field theory directly in three dimensions. The four-loop expansions of the  $\beta$ -functions are calculated for arbitrary  $N$ . The critical dimensionality  $N_c = 2.89 \pm 0.02$  and the stability matrix eigenvalues estimates obtained on the basis of the generalized Padé-Borel-Leroy resummation technique are shown to be in a good agreement with those found recently by exploiting the five-loop  $\varepsilon$ -expansions.

(1 December 1999)

Published in: *J. Phys. A: Math. and Gen.* **33** (2000) 3121-3135.

*Typeset using L<sup>A</sup>T<sub>E</sub>X*

---

\*E-mail address: feop@eltech.ru

# 1 Introduction

The study of the critical properties of magnetic phase transitions in three dimensional (3D) cubic crystal is a problem attracting theoretical efforts over more than 25 years. By using the lower-order renormalization-group (RG) approach, Wilson and Fisher [1], Aharony [2], and Ketley and Wallace [3, 4] showed that in the critical region the fluctuation instability of continuous phase transitions may be observed, and that it may lead to the isotropization of the system with a cubic anisotropy. This fact gave rise to the question of what regime of the critical behaviour is actually realized in 3D cubic crystal with  $N = 3$ . It was soon understood that the calculation of the critical dimensionality  $N_c$  of the order parameter is the crucial point in studying critical phenomena in a cubic crystal. Indeed, the critical value  $N_c$  separates two different regimes of critical behaviour of the system. For  $N > N_c$  the cubic rather than the isotropic fixed point is stable in 3D. At  $N = N_c$  the points interchange their stability so that for  $N < N_c$  the stable fixed point is the isotropic one. However, attempts to evaluate the critical dimensionality resulted in dramatically different estimates.

In fact, the one-loop RG analysis of the stability matrix eigenvalues of the cubic and isotropic fixed points as well as some symmetry arguments (see section 2) predicts that  $N_c$  should lie between 2 and 4. Many years ago the three-loop expansion for  $N_c$  as a power series in  $\varepsilon$  was obtained [3]. Summation of that short series at  $\varepsilon = 1$  ( $D = 3$ ) by means of the Padé approximant  $[1/1]$  yielded the value  $N_c = 3.128$  [5], while making use of the Padé-Borel resummation method results in the estimate  $N_c = 3$ . In contrast to this, the value  $N_c = 2.3$  has been found on the basis of the variational modification of the Wilson recursion relation method in [6]. Later, however, Newman and Riedel showed by decoupling the infinite system of the recursion relations for the scaling fields and then solving them that for  $D = 3$   $N_c \sim 3.4$  [7]. At the same time, the classical technique of high-temperature expansions, under some circumstances, allowed one to establish that for  $N = 3$  the isotropic critical asymptotics in a cubic crystal is unstable [8], thus implying  $N_c < 3$ . Ten years ago the analysis of the critical behaviour of the (mn)-component field model, which has a good number of interesting applications to the phase transitions in real substances, has been carried out within the three-loop RG approach in three-dimensions. The calculation of the stability matrix eigenvalues for the cubic model ( $m = 1, n = 3$ ) provided the stability of the cubic fixed point in 3D, and the critical dimensionality turned out to be equal to 2.91 [9]. In agreement with this, the estimate  $N_c = 2.9$  was given in [10]. More recently, Kleinert and Schulte-Frohlinde calculated the RG functions for the cubic model in  $(4 - \varepsilon)$  dimensions up to five-loop order [11]. Summation of the critical dimensionality expansion with the help of the Pade approximant  $[2/2]$  gave the estimate  $N_c = 2.958$  [12].

The cubic fixed point eigenvalues found by means of a simple resummation algorithm of the Borel type, accounting for the large-order behaviour of the  $\beta$ -functions when the anisotropy parameter is very small [14], indicated that the cubic point is stable in 3D [15]. Finally, in the recent work Ref. [16] by using finite size scaling techniques and the high precision Monte Carlo (MC) simulation it has been suggested that  $N_c$  coincides with three exactly. Such strong scattering in the estimates of  $N_c$  motivated us to study this problem with particular care. Calculation of the critical dimensionality as well as the eigenvalue exponents for the cubic and isotropic fixed points by exploiting the higher-order RG approach in three dimensions and generalized Padé-Borel-Leroy (PBL) resummation technique is the main goal of the paper. As will be shown, our estimates for  $N_c$  and eigenvalues are in excellent agreement with recent results [15] obtained on the basis of the five-loop  $\varepsilon$ -expansions.

The layout of the paper is as follows. In the next section the model Hamiltonian is introduced and the massive field-theoretical RG procedure in fixed dimensions is formulated. The perturbative expansions for  $\beta$ -functions for generic  $N$  are then deduced up to the four-loop order. In section 3 the structure of the RG flows of the model are investigated and the fixed point locations are calculated using the generalized PBL resummation method. The eigenvalue exponents of the most intriguing  $O(N)$ -symmetric and cubic fixed points are evaluated for the physically significant case  $N = 3$  and the stability problem is solved. The numerical estimate of the critical dimensionality  $N_c$ , at which the topology of the flow diagram changes, is obtained by resumming both the four-loop RG expansions for the  $\beta$ -functions in 3D and the five-loop  $\varepsilon$ -expansion for  $N_c$  at  $\varepsilon = 1$ . In the conclusion the results of the investigation are discussed, along with the predictions and numerical estimates obtained earlier on the basis of the same or other theoretical approaches.

## 2 The model, RG procedure and $\beta$ -functions

We start from the fluctuation Hamiltonian

$$H = \int d^d x \left[ \frac{1}{2} (m_0^2 \varphi_i^2 + \partial_\mu \varphi_i \partial_\mu \varphi_i) + \frac{1}{4!} (u_0 G_{ijkl}^1 + v_0 G_{ijkl}^2) \varphi_i \varphi_j \varphi_k \varphi_l \right], \quad (1)$$

where  $\varphi_i$ ,  $i = 1, \dots, N$ , is the real vector order parameter field in fixed  $d$  and  $m_0^2$  is the linear measure of the temperature,  $u_0$  and  $v_0$  denote the "bare" coupling constants. The symmetrized tensors associated with isotropic and cubic interactions are

$$G_{ijkl}^1 = \frac{1}{3} (\delta_{ij} \delta_{kl} + \delta_{ik} \delta_{jl} + \delta_{il} \delta_{kj}), \quad G_{ijkl}^2 = \delta_{ij} \delta_{ik} \delta_{il} \quad (2)$$

respectively.

The model (1) has a number of interesting applications to the phase transitions in three-dimensional simple and complicated systems. Indeed, when  $N = 1$  Hamiltonian (1) describes the critical phenomena in pure spin system (Ising model), while for  $N = 2$  it corresponds to the anisotropic  $XY$  model describing structural phase transitions in ferroelectrics as ordering the two-component alloys [1, 17]. The magnetic and structural phase transitions in a cubic crystal are governed by model (1) as  $N = 3$ . In the replica limit  $N \rightarrow 0$  Hamiltonian (1) is known to determine the critical properties of weakly disordered quenched systems undergoing second-order phase transitions [18] with a specific set of critical exponents [19]. Finally, the case  $N \rightarrow \infty$  corresponds to the Ising model with equilibrium magnetic impurities [20]. In this limit the Ising critical exponent of specific heat  $\alpha$  changes its sign and takes the Fisher renormalization [21] together with  $\nu$  and  $\gamma$ :  $\alpha \rightarrow -\alpha/(1-\alpha)$ ,  $\nu \rightarrow \nu/(1-\alpha)$ ,  $\gamma \rightarrow \gamma/(1-\alpha)$ .

To calculate the  $\beta$ -functions normalizing conditions must be imposed on renormalized one-particle irreducible inverse Green functions

$$\Gamma_R^{(N)}(p; m, u, v; \Lambda; d) = Z_\varphi^{N/2} \Gamma^{(N)}(p; m_0, u_0, v_0; \Lambda; d)$$

given by corresponding Feynman diagrams,  $\Lambda$  is the ultraviolet momentum cut-off. Within the massive field-theoretical RG scheme [22] at zero external momenta and at the limit  $\Lambda \rightarrow \infty$  they are normalized in a conventional way [23]:

$$\begin{aligned} \Gamma_R^{(2)}(p, -p; m, u, v; d) \Big|_{p=0} &= m^2, \\ \frac{\partial}{\partial p^2} \Gamma_R^{(2)}(p, -p; m, u, v; d) \Big|_{p=0} &= 1, \\ \Gamma_{uR}^{(4)}(\{p_i\}; m, u, v; d) \Big|_{\{p_i\}=0} &= m^{4-d} u, \\ \Gamma_{vR}^{(4)}(\{p_i\}; m, u, v; d) \Big|_{\{p_i\}=0} &= m^{4-d} v, \end{aligned} \tag{3}$$

where  $m$ ,  $u$  and  $v$  are the renormalized mass and dimensionless coupling constants. The vertices  $\Gamma_u^{(4)}$ ,  $\Gamma_v^{(4)}$  are connected with the vertex function without external lines normalized at zero external momenta

$$\Gamma_{ijkl}^{(4)}(0) = \Gamma_u^{(4)} \cdot G_{ijkl}^1 + \Gamma_v^{(4)} \cdot G_{ijkl}^2.$$

From equations (3) the expansions for the renormalization constants  $Z_\varphi$ ,  $Z_u$  and  $Z_v$  may be obtained

$$\begin{aligned} Z_\varphi^{-1} &= \frac{\partial}{\partial p^2} \Gamma^{(2)}(p, -p; m_0, u_0, v_0), \\ Z_u^{-1} &= \frac{1}{u_0} \Gamma_u^{(4)}(0; m_0, u_0, v_0), \\ Z_v^{-1} &= \frac{1}{v_0} \Gamma_v^{(4)}(0; m_0, u_0, v_0). \end{aligned} \tag{4}$$

These constants relate the "bare" mass  $m_0$  and coupling constants  $u_0$  and  $v_0$  of the initial Hamiltonian (1) to the corresponding physical parameters

$$m_0^2 + \delta m_0^2 = m^2, \quad m = Z_\varphi \Gamma^{(2)}(p, -p; m_0, u_0, v_0),$$

$$u_0 = m^{4-d} \frac{Z_u}{Z_\varphi^2} u, \quad v_0 = m^{4-d} \frac{Z_v}{Z_\varphi^2} v. \quad (5)$$

With relations (5) taken into account, the  $\beta$ -functions can be calculated via the formulae

$$\begin{aligned} \frac{\partial \ln u_0}{\partial u} \beta_u + \frac{\partial \ln u_0}{\partial v} \beta_v &= (d-4), \\ \frac{\partial \ln v_0}{\partial u} \beta_u + \frac{\partial \ln v_0}{\partial v} \beta_v &= (d-4), \end{aligned} \quad (6)$$

where  $\beta_g \equiv \frac{\partial g}{\partial [\ln m]}$ ,  $g = \{u, v\}$ .

For each Feynman graph contributing to the RG functions the corresponding contractions are computed by the algorithm developed in Ref. [24]. The combinatorial factors as well as the integral values are known from Ref. [25]. After some work we obtain the four-loop expansions for the  $\beta$ -functions in three dimensions:

$$\begin{aligned} \beta_u &= u \left\{ 1 - u - \frac{6}{N+8} v + \frac{1}{(N+8)^2} \left[ 3 (2.024691 N + 9.382716) u^2 \right. \right. \\ &\quad + 44.444444 u v + 10.222222 v^2 \left. \right] - \frac{1}{(N+8)^3} \left[ 3 (0.449648 N^2 \right. \\ &\quad + 18.313459 N + 66.546806) u^3 + 3 (6.646878 N + 164.613849) u^2 v \\ &\quad + 3 (0.621889 N + 100.955929) u v^2 + 65.937285 v^3 \left. \right] \\ &\quad + \frac{1}{(N+8)^4} \left[ -(0.155646 N^3 - 35.820204 N^2 - 602.521231 N \right. \\ &\quad - 1832.206732) u^4 - 3 (1.352882 N^2 - 182.073890 N \\ &\quad - 2064.170701) u^3 v + 3 (27.250336 N + 2110.408809) u^2 v^2 \\ &\quad \left. \left. + 9 (1.291017 N + 308.599361) u v^3 + 495.005747 v^4 \right] \right\}, \quad (7) \end{aligned}$$

$$\begin{aligned} \beta_v &= v \left\{ 1 - \frac{1}{N+8} (12 u + 9 v) + \frac{1}{(N+8)^2} \left[ (3.407407 N + 54.814815) u^2 \right. \right. \\ &\quad + 92.444444 u v + 34.222222 v^2 \left. \right] - \frac{1}{(N+8)^3} \left[ -(1.251107 N^2 \right. \\ &\quad - 41.853902 N - 469.333970) u^3 + 9 (0.248784 N + 136.511768) u^2 v \\ &\quad + 957.781662 u v^2 + 255.929737 v^3 \left. \right] + \frac{1}{(N+8)^4} \left[ (0.574653 N^3 \right. \\ &\quad - 0.267107 N^2 + 584.287672 N + 5032.692260) u^4 + 3 (0.057375 N^2 \\ &\quad + 107.641680 N + 5989.283536) u^3 v + 3 (7321.464604 \\ &\quad \left. \left. - 16.494003 N) u^2 v^2 + 11856.956858 u v^3 + 2470.392521 v^4 \right] \right\}. \quad (8) \end{aligned}$$

These equations are known to have four solutions corresponding to the trivial Gaussian, the Ising, the isotropic (Heisenberg) and the cubic fixed

points [2]. The most intriguing of them are the isotropic and cubic ones. The one-loop approximation analysis of the eigenvalue exponents for these points yields the upper boundary value for the critical dimensionality  $N_c$ ,  $N_c = 4$ .

To determine the lower boundary of  $N_c$  one should attract the specific symmetry property of model (1), when  $N = 2$  [26]. Namely, the transformation of the field components

$$\varphi_1 \rightarrow \frac{1}{\sqrt{2}} (\varphi_1 + \varphi_2) , \quad \varphi_2 \rightarrow \frac{1}{\sqrt{2}} (\varphi_1 - \varphi_2) \quad (9)$$

combined with substitution of the quartic couplings

$$u \rightarrow u + \frac{3}{2} v , \quad v \rightarrow -v \quad (10)$$

does not change the structure of the initial Hamiltonian itself. As a result, the  $\beta$ -functions (7), (8) should obey certain symmetry relations [27]:

$$\begin{aligned} \beta_u \left( u + \frac{3}{2} v, -v \right) &= \beta_u(u, v) + \frac{3}{2} \beta_v(u, v) , \\ \beta_v \left( u + \frac{3}{2} v, -v \right) &= -\beta_v(u, v) , \end{aligned} \quad (11)$$

but their form remain unchanged. However, for  $N = 2$  transformations (9) and (10) result in the relocation of the coupling constants values so that the cubic and Ising fixed points are transformed into each another at the 3D RG flow diagram. Since the exact RG equations always have the Ising fixed point, which inevitably is the saddle-knot one, these equations should also have the cubic fixed point, which will be unstable. In this situation, the isotropic fixed point, again always existing in the exact RG equations, should be the stable knot only. Therefore, we conclude that the lower boundary of  $N_c$  is not less than two. The real value of  $N_c$  can be obtained only on the basis of analysis of the RG flow diagram structure, provided the  $\beta$ -functions of the model are calculated in sufficiently high-order RG approximations and then processed by appropriate resummation techniques.

### 3 Resummation, fixed points and stability

It is well known that the field-theoretical RG series are divergent. The character of their large-order behaviour is well established only for simple  $O(N)$ -symmetric models [28, 29, 30]. The coefficients of the series at large  $k$  were shown to behave as  $c(-a)^k k! k^b$ , where the asymptotic parameters  $a$ ,  $b$  and  $c$  are assumed to be calculated for each RG function. Knowledge of the exact

values of the asymptotic parameters in combination with the most powerful resummation procedure of the Borel transformation with a conformal mapping, first proposed in Ref. [31], made it possible to develop the accomplished quantitative theory of critical behaviour of simple systems [32, 33].

At the same time, the asymptotic nature of RG functions of anisotropic models is still unknown. Calculating the large-order asymptotic behaviour for the series in such models is a very difficult problem. That is why, lacking any information about the large-order behaviour either the simple Padé-Borel or Chisholm-Borel resummation procedures are used. The latter technique, however, possesses at least two inherent drawbacks. First, some ambiguity in the calculation of coefficients of denominators of the Chisholm approximants is unavoidable [34]. Second, the Chisholm-Borel procedure does not hold the specific symmetry properties of a model. At the same time, exploiting the Borel transformation in combination with the Padé or Chisholm approximants shows that the results of calculation are very sensitive to the choice of the type of approximants. This may lead to estimates which do not provide reliable predictions even in the higher-loop RG approximations [35]. Besides, in the framework of both schemes it is very difficult to determine any error bounds for the evaluated quantities.

In this paper we attempt to overcome the outlined difficulties by applying the PBL resummation method, generalized for the two coupling constant case, to processing the RG expansions (7) and (8). This method, first introduced by Baker *et al* in [36], turned out to be highly efficient when used to study the critical behaviour of the simple  $O(N)$ -symmetric models in 3D. The critical exponent estimates obtained within the framework of this technique are regarded nowadays as the most accurate values, as those of [31, 32, 37]. We motivate our choice of the PBL resummation method with the following reasons.

- 3D RG expansions for the  $\beta$ -functions of the cubic model alternate in signs. Therefore, using PBL resummation technique is quite natural.
- It can be expected that for complex models with more than one coupling constant, the asymptotics of the RG series at large orders will include a factor  $k!k^b$ . The PBL resummation method removes divergences of this type.
- The PBL resummation method allows one to determine the error bounds for the physical quantities to be calculated, in a natural way.

The generalized PBL resummation procedure consists of the following. Let a physical quantity  $F(u, v)$  be represented by a double series

$$F(u, v) = \sum_{i,j} f_{ij} u^i v^j, \quad (12)$$

where coefficients  $f_{ij} \sim (i+j)!(i+j)^b$  at large orders ( $i, j \rightarrow \infty$ ), the additional parameter  $b$  being an arbitrary non-negative number to be defined below. Associated with the initial series (12) is the function

$$\mathcal{F}(u, v; b) = \int_0^\infty e^{-t} t^b B(ut, vt) dt \quad (13)$$

The Borel-Leroy transform  $B(x, y)$  is the analytical continuation of its Taylor series

$$B(x, y) = \sum_{ij} \frac{f_{ij}}{\Gamma(i+j+b+1)} x^i y^j \quad (14)$$

which is absolutely convergent in a circle of non-zero radius. In order to calculate the integral in (13) one should continue analytically  $B(x, y)$  for  $0 \leq x < \infty$  and  $0 \leq y < \infty$ . To this end, the rational Padé approximants  $[L/M]$  ( $x, y$ ) are used. The Padé approximant method is determined in a conventional way [13]. Let us consider a "resolvent" series

$$\tilde{B}(x, y, \lambda) = \sum_{k=0}^\infty \lambda^k \sum_{l=0}^k \frac{f_{l, k-l} x^l y^{k-l}}{\Gamma(k+b+1)} = \sum_{k=0}^\infty A_k \lambda^k, \quad (15)$$

where coefficients  $A_k$  are uniform polynomials of  $k$ th order in  $u$  and  $v$ . The sum of the series is then approximated by

$$B(x, y) = [L/M] \Big|_{\lambda=1}. \quad (16)$$

The Padé approximants  $[L/M]$  in  $\lambda$  are given by

$$[L/M] = \frac{P_L(\lambda)}{Q_M(\lambda)}, \quad (17)$$

where  $P_L(\lambda)$  and  $Q_M(\lambda)$  are polynomials of degrees  $L$  and  $M$ , respectively, with coefficients depending on  $x$  and  $y$  which should be determined from the conditions

$$\begin{aligned} Q_M(\lambda) \tilde{B}(x, y; \lambda) - P_L(\lambda) &= O(\lambda^{L+M+1}), \\ Q_M(0) &= 1. \end{aligned} \quad (18)$$

Replacing variables  $x = ut$  and  $y = vt$  in the Padé approximants and then evaluating the Borel-Leroy integral

$$\mathcal{F}(u, v; b) = \int_0^\infty e^{-t} t^b [L/M] \Big|_{\lambda=1} dt \quad (19)$$



we obtain the approximate expressions for RG functions.

Among Padé approximants the diagonal ( $L = M$ ) or near-diagonal ones were proved to exhibit the best approximating properties [13]. However, as the degree of the denominator  $M$  increases, the number of possible poles of the approximant increases too. If some of the poles belong to the positive real semiaxis, the corresponding approximant should be rejected. Due to this the choice of "working" approximants, which might be used for analytical continuation of the Borel-Leroy image onto the complex cut plane, is largely limited. On the other hand, varying the free parameter  $b$  in the Borel-Leroy transformation (13) allows one to optimize the resummation procedure under the condition that the fastest convergence of the iteration process is achieved. So, taking into account the above-mentioned remarks, in order to find the locations of the fixed points we adopt the following scheme. For the fixed  $N$ , the  $\beta$ -functions are resummed by virtue of transformation (13) in the highest-loop orders by shifting the transformation parameter  $b$ . For an analytical continuation of the Borel-Leroy transforms  $B_u(u, v)$ ,  $B_v(u, v)$  over the cut plain the most appropriate Padé approximants  $[2/1]$ ,  $[3/1]$  and  $[2/2]$  are used. The locations of the fixed points are then determined for each  $b$  from the solution of the set of equations:  $\beta_u^{res}(u_c, v_c) = 0$ ,  $\beta_v^{res}(u_c, v_c) = 0$ . The "true" locations are obtained by averaging over the values given by the approximants under the optimal value of the parameter  $b$ , at which the quantity  $|1 - \mathcal{F}_L(u, v; b) / \mathcal{F}_{L-1}(u, v; b)|$  reaches its local minima. The quantity  $\mathcal{F}_L(u, v; b)$  is evaluated for the  $L$ -partial sum of the series in equation (19), where  $L$  denotes the step of truncation of the series.

The results of the computation of the cubic fixed point locations depending on the parameter  $b$  are presented for the physically important case  $N = 3$  in figure 1. Three curves correspond to the three Padé approximants. The parameter  $b$  shifts from 0 to 3. As can be seen from the figure the optimal value of  $b$  is zero. At this point the numerical values of the cubic fixed point locations given by different approximants are the closest to each other. The result of computing the cubic fixed point locations for  $N = 3$  are also presented in table 1. In the first three columns of the table the fixed point locations values found by means of the Padé approximants  $[2/1]$ ,  $[3/1]$ , and  $[2/2]$  at  $b = 0$  are given. Averaging the results of processing over all of the approximants under the optimal value of  $b$  gives the estimates presented in the fourth column of the table. We adopt these numbers as the final estimates for the cubic fixed point locations found within the four-loop approximation. As the degree of accuracy for these approximate values we take the maximum deviations of the average values of the fixed point locations from those given by the approximants at  $b = 0$ .

One can observe, looking at figure 1, that the values of the cubic fixed point locations given by the symmetric approximant  $[2/2]$  depend weakly on the shift parameter  $b$ . Averaging over all the values given by this approximant

within the interval  $[0,3]$  results in the cubic fixed point locations estimates presented in the fifth column of table 1. The coordinates of the cubic fixed point found earlier on the basis of the three- and four-loop approximations, using the Chisholm-Borel resummation method, are presented in the table, for comparison. These numbers include the normalizing multiplier  $\frac{11}{9}$  needed to compare our  $\beta$ -functions with those obtained in [9, 10].

To verify the correctness of the chosen approach let us apply the above considered scheme to estimate the fixed point locations of the  $O(3)$ -symmetric model for which the numerical results are well known. The six-loop 3D RG expansion for the  $\beta$ -function of this model was reported in [31, 36]. The PBL resummation of that series using eight types of Padé approximants  $[2/1]$ ,  $[3/1]$ ,  $[2/2]$ ,  $[4/1]$ ,  $[3/2]$ ,  $[5/1]$ ,  $[4/2]$  and  $[3/3]$  yields, after solving the equation  $\beta^{res}(g_c) = 0$ , the picture displayed in figure 2. It is seen that the values of the isotropic fixed point location calculated in the highest RG orders with the help of the approximants  $[3/3]$ ,  $[4/2]$  and  $[3/2]$  are very weakly dependent on the parameter  $b$  varied within the interval  $0 \leq b \leq 15$ . The curves corresponding to these approximants are intersected at the point  $b = 4.5$ . Therefore  $b = 4.5$  is the optimal value of the transformation parameter for which the fastest convergence of the iteration procedure is ensured. For  $b = 4.5$  the central value estimate of the isotropic fixed point is  $g_c = 1.392$ . The maximum deviation of the central value from the values given by some of the approximants  $[3/3]$ ,  $[4/2]$  and  $[3/2]$  at the point  $b = 10$  is adopted approximately as an apparent accuracy of the calculation,  $\Delta = 0.0013$ . Such a small error can be explained by the small dispersion of the curves within the range  $5 \leq b \leq 10$ . So, the estimate  $g_c = 1.3920 \pm 0.0013$  is in excellent agreement with those found more then 20 years ago in [31, 36] as well as with recent results of [32].

Within the framework of the four-loop approximation there are only three appropriate Padé approximants. Averaging the results of computing the isotropic fixed point location given by the approximants  $[2/1]$ ,  $[3/1]$  and  $[2/2]$  under the optimal value of the transformation parameter results in the estimate  $g_c = 1.3925 \pm 0.0070$ . The error was determined again through the maximum deviation of the central value from those given by each of the approximants at  $b = 0$ . It is seen that the four-loop estimate of the coordinate of the isotropic fixed point is in a good accordance with the best ones followed from the six-loop consideration.

Note, however, that the coordinate of the  $O(3)$ -symmetric fixed point calculated within the five-loop approximation does not approach the "exact" value. Namely, the PBL resummation procedure leads to the estimate  $g_c = 1.3947 \pm 0.0040$ . Although the error of the calculation became visibly smaller, the central value of the fixed point location stepped aside from the four- and six-loop ones.

Thus, the fulfilled numerical analysis shows that the isotropic fixed point

location estimate obtained in the four-loop level occurs close to the six-loop value. One can expect, therefore, that in the case of the cubic model the fixed point locations  $u_c = 1.3428 \pm 0.0200$ ,  $v_c = 0.0815 \pm 0.0300$  (fourth column of table 1) will not be strongly distinguish from the "exact", say, the six-loop, values. The coordinates of the cubic fixed point for some  $N$  are presented in table 2. Our calculations show that for  $N = 3$  the coordinates of the cubic fixed point practically do not differ from those of the Heisenberg one. However, with increasing  $N$  the cubic fixed point runs away from the isotropic point moving towards the Ising one. In the large  $N$  limit these two fixed points become close to each another so much that the influence of the  $O(N)$ -symmetric invariant on the critical thermodynamics of the cubic model vanishes. This can be easily seen by applying the  $\frac{1}{N}$  consideration to the one-loop solutions of the RG equations of model (1). Indeed, rescaling the coupling constants  $u \rightarrow u/N$ ,  $v \rightarrow v/N$  in the initial Hamiltonian and taking then the limit  $N \rightarrow \infty$  one can see that the cubic fixed point approaches the Ising one asymptotically. So, the cubic model turns out to be split into  $N$  non-interacting Ising models, the critical behaviour of each of them will be determined by a set of the critical exponents renormalized according to Fisher [21].

Another way to determine the fixed point locations in fixed  $D$  is to construct the RG flows diagram of the model. If, at the flows diagram, there exists a fixed point of stable knot type, the trajectories originated from some point within the range of stability of the initial Hamiltonian would flow towards the knot. The region at the flow diagram where the trajectories are intersected provides the coordinates of the stable fixed point. Investigating the 3D RG flow diagram of model (1) in the four-loop approximation we arrive at the conclusion that the cubic rather than the isotropic fixed point is absolutely stable for all  $N \geq 3$ .

At the same time, the reliable prediction about the stability of the cubic fixed point for  $N \geq 3$  can be made on the basis of calculating the eigenvalue exponents  $\lambda$ 's of the stability matrix

$$M_{ij} = \begin{pmatrix} \frac{\partial \beta_u}{\partial u} & \frac{\partial \beta_u}{\partial v} \\ \frac{\partial \beta_v}{\partial u} & \frac{\partial \beta_v}{\partial v} \end{pmatrix}$$

taken at  $u = u_c$  and  $v = v_c$ . If the real parts of both eigenvalues are negative, the fixed point is the stable knot in the  $(u, v)$  plane. If  $\lambda_1, \lambda_2$  have opposite signs, the point is of the "saddle-knot" type.

To calculate the stability matrix eigenvalues of the cubic and isotropic fixed points we have chosen the following strategy. First, the derivatives of the  $\beta$ -functions (7) and (8) are calculated, and the new RG expansions resummed by means of the PBL technique are substituted into the matrix  $M_{ij}$ . The eigenvalue exponents of the matrix of derivatives  $M_{ij}$  obtained in such a way are then evaluated under the optimal value of the transformation

parameter  $b$ . In figure 3 we present our numerical results for the series  $-\frac{\partial\beta_u}{\partial u}$  and  $-\frac{\partial\beta_v}{\partial v}$  for the physically interesting case  $N = 3$ . The curves correspond to the three types of the Padé approximants used within the four-loop approximation. The crossing of the curves gives the optimal value of  $b$  at which we find  $\frac{\partial\beta_u}{\partial u}|_{opt} = -0.7536$  and  $\frac{\partial\beta_v}{\partial v}|_{opt} = -0.0331$ . Because the series  $-\frac{\partial\beta_u}{\partial u}$  and  $-\frac{\partial\beta_v}{\partial v}$  turn out to be shorter by one order in comparison with  $-\frac{\partial\beta_u}{\partial u}$  and  $-\frac{\partial\beta_v}{\partial v}$ , their resummings performed with the help of the approximant  $[2/1]$  only yields the monotonic dependence of the result of processing on the parameter  $b$ . In this unfavorable situation, we take into account an additional Padé approximant  $[1/1]$  to optimize the iteration procedure. The results are plotted in figure 4. For the optimal values of  $b$  we obtain  $\frac{\partial\beta_u}{\partial v}|_{opt} = -0.4566$  and  $\frac{\partial\beta_v}{\partial u}|_{opt} = -0.0409$ . Straightforward calculation of the eigenvalues of the stability matrix  $M_{ij}$  gives for the cubic fixed point the numbers provided in table 3. The eigenvalues of the isotropic fixed point as well as the analogous numerical estimates obtained recently in [15] on the basis of using the five-loop  $\varepsilon$ -expansions are presented for comparison therein. These estimates show that the cubic fixed point is absolutely stable in 3D for  $N = 3$  while the isotropic fixed point appears to be stable on the  $u$ -axis only. Our numerical results agree well with those obtained in [15]. Unfortunately, at present we cannot indicate realistic error bounds in our calculation of the stability matrix eigenvalues. Nevertheless, a crude estimate can be done. In fact, if the model (1) is almost identical to some marginal system for which  $N_c = 3$  in 3D, the stability index  $\lambda_2$  both for the isotropic and for the cubic fixed points should be equal to zero at  $N = 3$  and, consequently, the points should coincide. Therefore, as can be seen from the numbers given in table 3, the four-loop approximation predicts eigenvalues with error about 0.01. Of course, dealing with the theory without a small parameter and the short perturbative expansions one would refer to such a level of accuracy as satisfactory. However numerically small errors may lead, sometimes, to qualitatively incorrect results [35].

Note, that although the recent high precision MC simulation using finite size scaling techniques [16] predicts the stability of the isotropic rather than the cubic fixed point, the absolute value of the stability eigenvalue  $|\lambda_2|$  obtained for the isotropic point turned out to be very small. This is in accordance with our estimate.

Let us now calculate the critical dimensionality  $N_c$  of the order parameter field. The critical dimensionality is defined as a value of  $N$  at which the cubic fixed point coincides with the isotropic one. Equivalently, for  $N = N_c$  the second eigenvalue of the stability matrix  $M_{ij}$  vanishes,  $\lambda_2 = 0$ . Studying carefully the 3D RG flow diagram of model (1) depending on the order of approximation for different Padé approximants we arrive at the conclusion that  $N_c = 2.910 \pm 0.035$  and  $N_c = 2.890 \pm 0.020$  within the three- and four-

loop approximations, respectively. The accuracy of the calculation of  $N_c$  was determined through the evaluation of the stability matrix eigenvalues for different  $N$  from the interval of errors mentioned above. That value of  $N = N_c$ , above or below its central number, at which the second eigenvalue  $\lambda_2$  was becoming non-zero, was taking for the upper or lower boundary of  $N_c$ , respectively.

It is worth comparing the four-loop estimate of  $N_c$  just found with that which can be obtained within the  $\varepsilon$ -expansion method. The five-loop  $\varepsilon$ -expansion for  $N_c$  has been calculated in [11]. The series turned out to be alternating in signs that allows one to resum it by means of the PBL technique. To this end, we use again the most appropriate Padé approximants  $[2/1]$ ,  $[3/1]$  and  $[2/2]$  for analytical continuation of the Borel-Leroy transform for all  $0 \leq \varepsilon t \leq \infty$ . Dependence of the results of processing of the critical dimensionality  $N_c$  on the transformation parameter  $b$  is depicted in figure 5. The curves corresponding to the approximants are crossed at the point  $b \sim 1$ . The appropriate value of the critical dimensionality is  $N_c = 2.894 \pm 0.040$ . As an error of the calculation it is natural to assume the maximum scattering of numerical values given by the approximants at  $b = 0$  from that obtained at the crossing point of the curves. This estimate of  $N_c$  is in excellent accordance with the above found within the 3D RG approach. It also agrees well with the estimates obtained earlier on the basis of the different resummation technique [9, 10]. So, both schemes, the RG technique directly in 3D and the  $\varepsilon$ -expansion method, result in the same estimate of the critical dimensionality  $N_c = 2.89$ , thus implying that the cubic fixed point is stable in three dimensions for  $N \geq 3$ . This means that the critical behaviour of the magnetic phase transitions in crystals with cubic anisotropy should belong to the cubic rather than the isotropic universality class with a certain set of critical exponents. However, due to the obvious marginality of the model ( $N_c \sim 3$ ) and closeness of both (isotropic and cubic) fixed points on the 3D RG flow diagram for  $N = 3$ , the critical exponents values of the cubic point will be practically the same of the isotropic one. That is why the calculation of the critical exponents in cubic magnets with  $N = 3$  seems to be of academic interest only.

## Conclusion

To summarize, the complete analysis of the global structure of RG flows of a model with two quartic coupling constants associated with isotropic and cubic interactions describing magnetic and structural phase transitions in a good number of real substances has been carried out within the massive field theory directly in three dimensions. Perturbative expansions for the  $\beta$ -functions were deduced for generic  $N$  up to four-loop order. The fixed points

locations were found for  $N \geq 3$  by applying the generalized Padé-Borel-Leroy resummation technique. On the basis of comparative numerical analysis with the  $O(N)$ -symmetric models, the fixed point locations for which have been solidly established [32, 33], we have made the assumption that the four-loop estimates of the cubic fixed point locations should not differ strongly from the "exact" values within the error bounds.

The analysis of the eigenvalue exponents of the isotropic and cubic fixed points fulfilled for the physically significant case  $N = 3$  has shown that the cubic rather than the isotropic fixed point is absolutely stable in 3D. The eigenvalues estimates (see table 3) were found to agree well with those calculated on the basis of exploiting the five-loop  $\varepsilon$ -expansions combined with a careful resummation procedure [15]. Our results agree numerically with the recent high precision MC estimates [16], in spite of the latter predicting the stability of the isotropic rather than the cubic fixed point.

The critical dimensionality  $N_c$  of the order parameter, at which the topology of the flow diagram changes, has been estimated by the two different methods: (a) by resumming the four-loop RG expansions for the  $\beta$ -functions in 3D and (b) by resumming the five-loop  $\varepsilon$ -expansion for  $N_c$  at  $\varepsilon = 1$ . The numerical estimates  $N_c = 2.89 \pm 0.02$  and  $N_c = 2.894 \pm 0.040$  obtained are in a good agreement with the earlier results [9, 10] and confirm the conclusion about the stability of the cubic fixed point for  $N \geq 3$ . Consequently, the magnetic and structural phase transitions in three-dimensional anisotropic crystals with cubic symmetry are of second order and their critical thermodynamics should be governed by the cubic fixed point with a certain set of critical exponents. Unfortunately, the cubic universality class is not easily distinguished experimentally from the isotropic one, due to the obvious marginality of the problem,  $N_c \sim 3$ .

## References

- [1] K. G. Wilson and M. E. Fisher, Phys. Rev. Lett. **28** (1972) 240; K. G. Wilson, Phys. Rev. Lett. **28** (1972) 548.
- [2] A. Aharony, Phys. Rev. **B8** (1973) 4270.
- [3] I. J. Ketley and D. J. Wallace, J. Phys. **A6** (1973) 1667.
- [4] D. J. Wallace, J. Phys. **C6** (1973) 1390. See also R. A. Cowley and A. D. Bruce, J. Phys. **C6** (1973) L191.
- [5] A. Aharony, A. D. Bruce, Phys. Rev. Lett. **33** (1974) 427; A. Aharony (unpublished).
- [6] M. C. Yalabik and A. Houghton, Phys. Lett. **A61** (1977) 1.

- [7] K. E. Newman and E. K. Riedel, Phys. Rev. **B25** (1982) 264.
- [8] M. Ferer, J. P. Van Dyke, and W. J. Camp, Phys. Rev. **B23** (1981) 2367.
- [9] N. A. Shpot, Phys. Lett. **A142** (1989) 474.
- [10] I. O. Mayer, A. I. Sokolov, and B. N. Shalaev, Ferroelectrics. **95** (1989) 93. In this article the four-loop RG expansions of the model are reported for the cases  $N = 0$  and  $N = 3$  only. Critical exponents estimates for the cubic fixed point have been obtained in three dimensions by making use of the simple Chisholm-Borel resummation method. However somewhat analysis for  $N_c$  as well as for the eigenvalue exponents of the cubic fixed point has not been given.
- [11] H. Kleinert and V. Schulte-Frohlinde, Phys. Lett. **B342** (1995) 284.
- [12] It was established that the diagonal or near-diagonal Padé approximants exhibit the best approximating properties. See for instance [13]
- [13] G. A. Baker, Jr. and P. Graves-Morris, *Padé Approximants* (Reading, MA: Addison-Wesley) 1981.
- [14] H. Kleinert and S. Thoms, Phys. Rev. **D52** (1995) 5926.
- [15] H. Kleinert, S. Thoms, and V. Schulte-Frohlinde, Phys. Rev. **B56** (1997) 14428.
- [16] M. Caselle and M. Hasenbusch, J. Phys. **A31** (1998) 4603.
- [17] E. Brezin, J. C. Le Guillou, and J. Zinn-Justin, Phys. Rev. **B10** (1974) 892.
- [18] G. Grinstein, A. Luther, Phys. Rev. **B13** (1976) 1329; A. Aharony, Phys. Rev. **B13** (1976) 2092.
- [19] A. B. Harris and T. C. Lubensky, Phys. Rev. Lett. **33** (1974) 1540; T. C. Lubensky, Phys. Rev. **B11** (1975) 3573; D. E. Khmel'nitskii, Zh. Eksp. Teor. Fiz. **68** (1975) 1960 [Sov. Phys. JETP **41** (1976) 981]; B. N. Shalaev, Zh. Eksp. Teor. Fiz. **73** (1977) 2301 [Sov. Phys. JETP **46** (1977) 1204]; C. Jayaprakash, H. J. Katz, Phys. Rev. **B16** (1977) 3987.
- [20] A. Aharony, Phys. Rev. Lett. **31** (1973) 1494.
- [21] M. E. Fisher, Phys. Rev. **176** (1968) 257.
- [22] G. Parisi, in: *Proceedings of the Cargreese Summer School 1973* (unpublished); J. Stat. Phys. **23** (1980) 49.

- [23] E. Brezin, J. C. Le Guillou, and J. Zinn-Justin. Field theoretical approach to critical phenomena, in: *Phase Transitions and Critical Phenomena*, edited by C. Domb and M. S. Green. Vol. 6 (Academic Press, New York 1976).
- [24] A. I. Mudrov and K. B. Varnashev, Phys. Rev. **B57** (1998) 3562.
- [25] B. G. Nickel, D. I. Meiron, and G. A. Baker, Jr., *Compilation of 2-pt and 4-pt graphs for continuous spin model* (Report University of Guelph, 1977).
- [26] I. O. Mayer, A. I. Sokolov, Izv. Akad. Nauk SSSR, Ser. Fiz. **51** (1987) 2103.
- [27] A. L. Korzhenevskii, Zh. Eksp. Teor. Fiz. **71** (1976) 1434 [Sov. Phys. JETP **44** (1976) 751].
- [28] L. N. Lipatov, Zh. Eksp. Teor. Fiz. **72** (1977) 411 [Sov. Phys. JETP **45** (1977) 216].
- [29] E. Brezin, J. C. Le Guillou, and J. Zinn-Justin, Phys. Rev. **D15** (1977) 1544.
- [30] E. Brezin, G. Parisi, J. Stat. Phys. **19** (1978) 269.
- [31] J. C. Le Guillou and J. Zinn-Justin, Phys. Rev. Lett. **39** (1977) 95.
- [32] R. Guida and J. Zinn-Justin, J. Phys. **A31** (1998) 8103.
- [33] J. Zinn-Justin *Quantum Field Theory and Critical Phenomena*, Clarendon Press (Oxford 1989, third ed. 1996) and related articles in this book.
- [34] J. S. R. Chisholm, Math. Comput. **27** (1973) 841.
- [35] A. I. Sokolov and K. B. Varnashev, Phys. Rev. **B59** (1999) 8363. See also K. B. Varnashev, Phys. Rev. **B61** (2000) (at press); cond-mat/9909087.
- [36] G. A. Baker, Jr., B. G. Nickel, and D. I. Meiron, Phys. Rev. **B17** (1978) 1365.
- [37] J. C. Le Guillou and J. Zinn-Justin, Phys. Rev. **B21** (1980) 3976.



## Figure Captions

Fig. 1. Curves demonstrating the dependence of the results of calculating the cubic fixed point locations on the transformation parameter  $b$  for  $N = 3$ . The upper curve ( $\diamond$ ) corresponds to the  $[2/1]$  approximant, while the middle ( $\triangle$ ) and lower ( $\square$ ) curves correspond to the  $[2/2]$  and  $[3/1]$  approximants, respectively.

Fig. 2. The results of computation of the  $O(3)$ -symmetric fixed point locations from the three- to the six-loop approximations obtained on the basis of the PBL resummation method with eight types of the approximants:  $[2/1]$  -  $\diamond$ ,  $[3/1]$  -  $\square$ ,  $[2/2]$  -  $\triangle$ ,  $[4/1]$  - full  $\diamond$ ,  $[3/2]$  - full  $\triangle$ ,  $[5/1]$  - full  $\circ$ ,  $[4/2]$  -  $\circ$ ,  $[3/3]$  -  $\times$ .

Fig. 3. Graphs of dependence of the results of processing of the series a)  $-\frac{\partial\beta_u}{\partial u}$ , b)  $-\frac{\partial\beta_v}{\partial v}$  on the parameter  $b$ ,  $N = 3$ . The curves are given in the same notations as in the previous figures.

Fig. 4. Graphs of dependence of the results of processing of the series a)  $-\frac{\partial\beta_u}{\partial v}$ , b)  $-\frac{\partial\beta_v}{\partial u}$  on the parameter  $b$ ,  $N = 3$ . For the curves corresponding to the approximants  $[1/1]$  and  $[2/1]$  the notation  $\diamond$  and  $\square$  are used, respectively.

Fig. 5. Dependence of the results of processing of the  $\varepsilon$ -series for the critical dimensionality  $N_c$  on the transformation parameter  $b$ .

Table 1: Coordinates of the cubic fixed point of RG equations for  $N = 3$  found under the optimal value of the transformation parameter  $b = 0$ .

	[2/1]	[3/1]	[2/2]	Average value	Average over [2/2]
$u_c$	1.3536	1.3338	1.3410	$1.3428 \pm 0.0200$ $1.3480^a, 1.3357^b$	1.3425
$v_c$	0.0526	0.1026	0.0894	$0.0815 \pm 0.0300$ $0.0904^a, 0.0906^b$	0.0937

<sup>a</sup> Quoted from Ref. [9]

<sup>b</sup> Quoted from Ref. [10]

Table 2: Coordinates of the cubic fixed point of RG equations for some  $N$  found under the optimal value of the transformation parameter  $b$  within the four-loop approximation. The average values of the coordinates calculated over the most stable Padé approximant [2/2] are also presented for comparison.

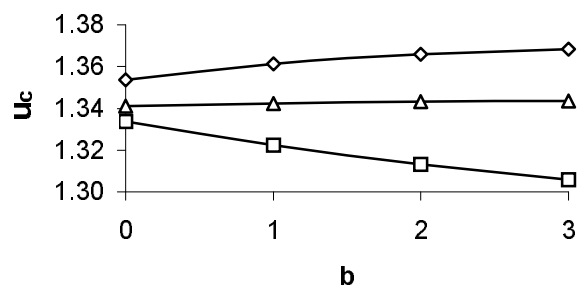
N	4	5	6	7	8	9	10
$u_c$	0.9055	0.6980	0.5807	0.5060	0.4544	0.4168	0.3881
$v_c$	0.8167	1.2361	1.5386	1.7874	2.0076	2.2108	2.4032
$u_c$ [2/2]	0.8981	0.6886	0.5708	0.4962	0.4448	0.4074	0.3789
$v_c$ [2/2]	0.8380	1.2608	1.5649	1.8148	2.0359	2.2400	2.4333

Table 3: Four-loop eigenvalue exponents estimates for the cubic (CFP) and isotropic (IFP) fixed points found for  $N = 3$  under the optimal value of the transformation parameter  $b$ .

	CFP	CFP, Ref. [15]	IFP	IFP, Ref. [15]
$\lambda_1$	-0.7786	-0.7648	-0.7791	-0.7640
$\lambda_2$	-0.0081	-0.0085	0.0077	0.0089

Fig. 1

a)



b)

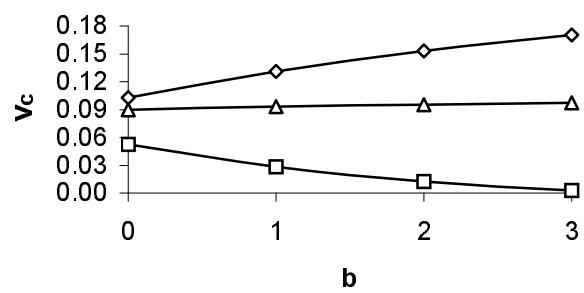


Fig. 2

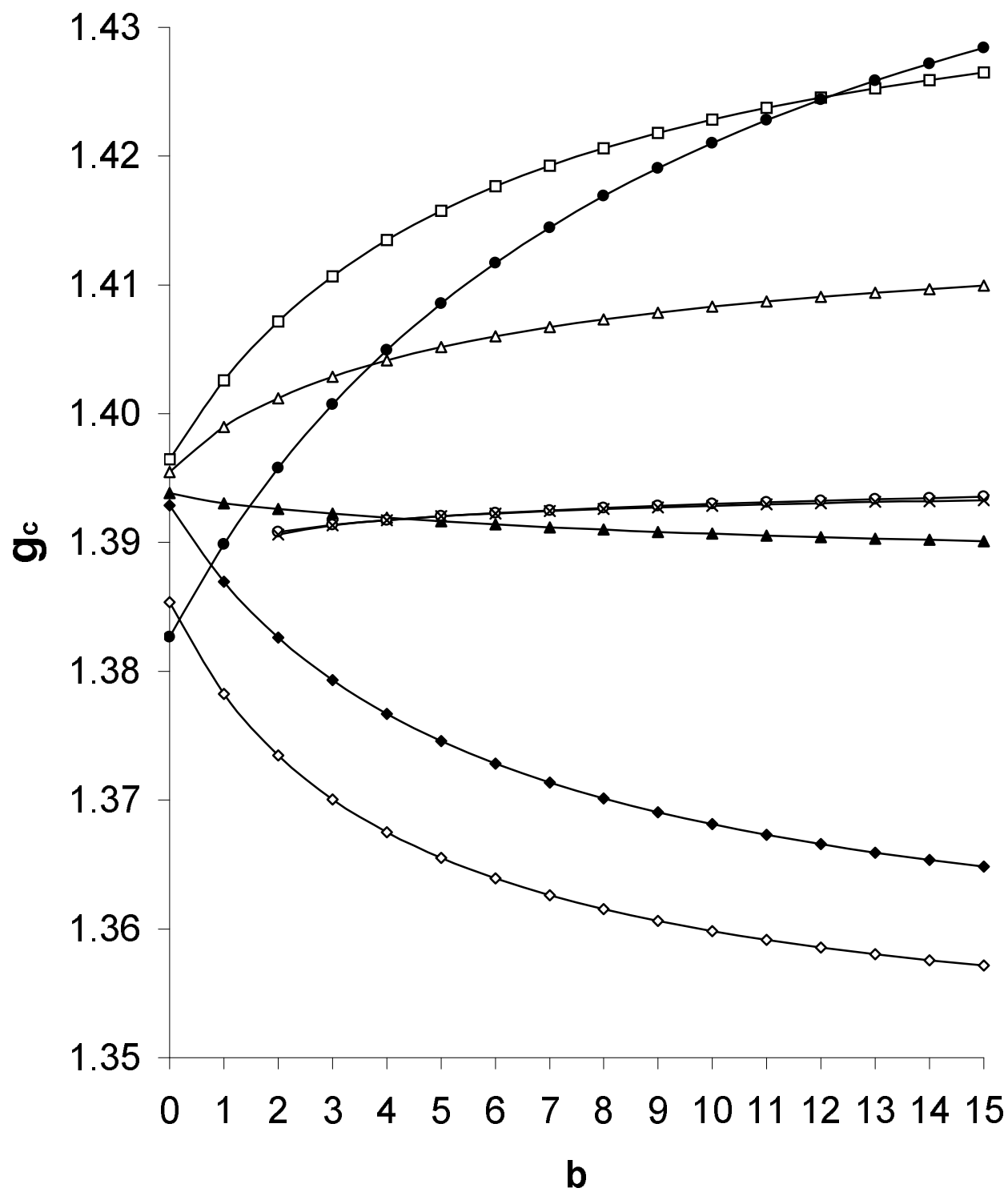
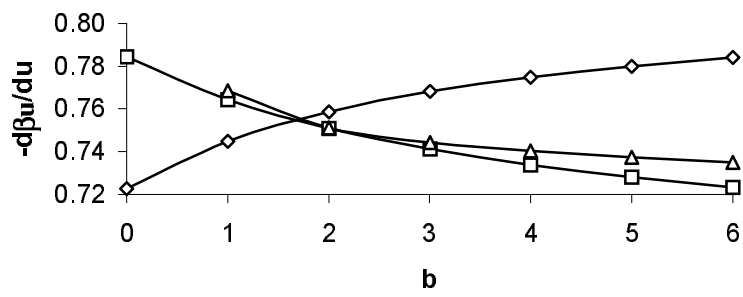


Fig. 3

a)



b)

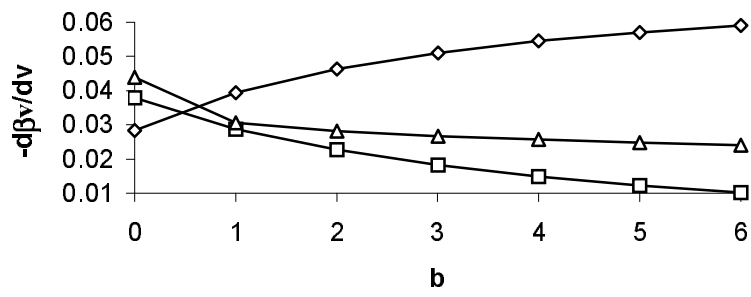
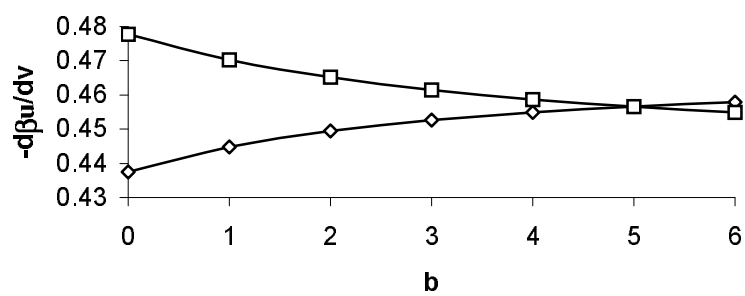


Fig. 4

a)



b)

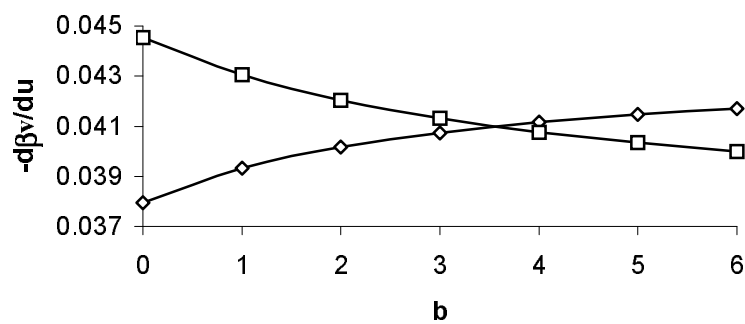


Fig. 5

